NASA/TM–2001–210862

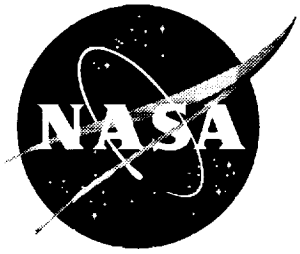

An Implicit Characteristic Based Method for Electromagnetics

John H. Beggs
Langley Research Center, Hampton, Virginia

W. Roger Briley
Mississippi State University, Mississippi State, Mississippi

May 2001

The NASA STI Program Office ... in Profile

Since its founding, NASA has been dedicated to the advancement of aeronautics and space science. The NASA Scientific and Technical Information (STI) Program Office plays a key part in helping NASA maintain this important role.

The NASA STI Program Office is operated by Langley Research Center, the lead center for NASA's scientific and technical information. The NASA STI Program Office provides access to the NASA STI Database, the largest collection of aeronautical and space science STI in the world. The Program Office is also NASA's institutional mechanism for disseminating the results of its research and development activities. These results are published by NASA in the NASA STI Report Series, which includes the following report types:

- TECHNICAL PUBLICATION. Reports of completed research or a major significant phase of research that present the results of NASA programs and include extensive data or theoretical analysis. Includes compilations of significant scientific and technical data and information deemed to be of continuing reference value. NASA counterpart of peer-reviewed formal professional papers, but having less stringent limitations on manuscript length and extent of graphic presentations.

- TECHNICAL MEMORANDUM. Scientific and technical findings that are preliminary or of specialized interest, e.g., quick release reports, working papers, and bibliographies that contain minimal annotation. Does not contain extensive analysis.

- CONTRACTOR REPORT. Scientific and technical findings by NASA-sponsored contractors and grantees.

- CONFERENCE PUBLICATION. Collected papers from scientific and technical conferences, symposia, seminars, or other meetings sponsored or co-sponsored by NASA.

- SPECIAL PUBLICATION. Scientific, technical, or historical information from NASA programs, projects, and missions, often concerned with subjects having substantial public interest.

- TECHNICAL TRANSLATION. English-language translations of foreign scientific and technical material pertinent to NASA's mission.

Specialized services that complement the STI Program Office's diverse offerings include creating custom thesauri, building customized databases, organizing and publishing research results... even providing videos.

For more information about the NASA STI Program Office, see the following:

- Access the NASA STI Program Home Page at ***http://www.sti.nasa.gov***

- E-mail your question via the Internet to help@sti.nasa.gov

- Fax your question to the NASA STI Help Desk at (301) 621-0134

- Phone the NASA STI Help Desk at (301) 621-0390

- Write to:
  NASA STI Help Desk
  NASA Center for AeroSpace Information
  7121 Standard Drive
  Hanover, MD 21076-1320

NASA/TM–2001–210862

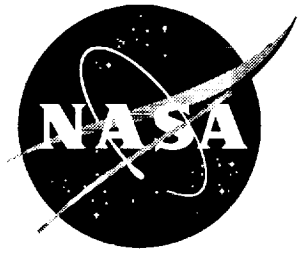

An Implicit Characteristic Based Method for Electromagnetics

John H. Beggs
Langley Research Center, Hampton, Virginia

W. Roger Briley
Mississippi State University, Mississippi State, Mississippi

National Aeronautics and
Space Administration

Langley Research Center
Hampton, Virginia 23681–2199

May 2001

Available from:

NASA Center for AeroSpace Information (CASI)
7121 Standard Drive
Hanover, MD 21076 1320
(301) 621-0390

National Technical Information Service (NTIS)
5285 Port Royal Road
Springfield, VA 22161-2171
(703) 605-6000

Abstract

An implicit characteristic-based approach for numerical solution of Maxwell's time-dependent curl equations in flux conservative form is introduced. This method combines a characteristic based finite difference spatial approximation with an implicit lower-upper approximate factorization (LU/AF) time integration scheme. This approach is advantageous for three-dimensional applications because the characteristic differencing enables a two-factor approximate factorization that retains its unconditional stability in three space dimensions, and it does not require solution of tridiagonal systems. Results are given both for a Fourier analysis of stability, damping and dispersion properties, and for one-dimensional model problems involving propagation and scattering for free space and dielectric materials using both uniform and nonuniform grids. The explicit FDTD algorithm is used as a convenient reference algorithm for comparison. The one-dimensional results indicate that for low frequency problems on a highly resolved uniform or nonuniform grid, this LU/AF algorithm can produce accurate solutions at Courant numbers significantly greater than one, with a corresponding improvement in efficiency for simulating a given period of time. This approach appears promising for development of LU/AF schemes for three dimensional applications.

1 Introduction

1.1 Background

In the regime of finite-difference solutions for Maxwell's time dependent curl equations, explicit methods such as the Finite-Difference Time-Domain (FDTD) method [1]–[4], the Transmission Line Method (TLM), or (more recently) Finite-Volume Time-Domain (FVTD) methods have been standard techniques for the past 20-30 years. These methods are relatively simple and efficient, and have proven very robust and adequate for many types of problems.

Since these explicit methods are conditionally stable, their maximum time step is limited by a stability constraint that depends on the local grid spacing. The conditional stability restriction can increase the cost of analyzing electromagnetic (EM) problems, especially when nonuniform grids are needed, because a small local grid structure can require a time step smaller than would otherwise be required to accurately resolve the physical wave propagation. On the other hand, implicit algorithms can provide unconditional stability which allows the time step to be selected for accuracy and resolution of the frequency content of the excitation sources, without a stability restriction.

Implicit algorithms were first proposed for electromagnetics by Holland [5]. They have not received widespread use in electromagnetics, however, perhaps due to increased complexity and in some cases the need to solve a linear system of equations. For example, centered spatial difference approximations in conjunction with alternating direction implicit (ADI) schemes require the solution of (for example) tridiagonal systems for each coordinate direction. Furthermore, although this type of scheme is unconditionally stable for the first-order wave equation in two dimensions, it is known to be unconditionally unstable in three dimensions [6]. The usual Fourier stability analysis does not account for nonperiodic boundary conditions, however, and it has been shown using a matrix stability analysis that this three dimensional centered difference algorithm is conditionally

stable when used with upwind boundary conditions [7].

There has been recent work to develop characteristic based explicit and implicit algorithms for CEM that are related to some solution algorithms from computational fluid dynamics. These methods have been developed for curvilinear three dimensional grids, using both finite difference and finite volume approximations. Shankar et al. [8], [9] developed explicit characteristic-based finite-volume methods, using both flux-vector and flux-difference splittings for electromagnetics. Shang, et. al. [10]–[19] have developed both implicit and explicit characteristic based methods. Shang [10]–[11] developed an implicit characteristic based ADI method that leads to simple bidiagonal systems that are easily solved, rather than tridiagonal or pentadiagonal systems. This characteristic-based scheme is unconditionally stable in two dimensions and conditionally stable in three dimensions [11]. Shang and Fithen [18] also developed characteristic based finite difference and finite volume schemes using Runge-Kutta time integration, in curvilinear coordinates. Gaitonde and Shang [20] and Turkel [4] have recently explored high order accurate compact differencing schemes that require tridiagonal solutions for spatial approximations, whether implicit or explicit time integration is used. Turkel [4] has suggested a two dimensional implicit version based on an ADI scheme. More recent work includes development of two and three-dimensional implicit ADI FDTD schemes [21]–[24]. However, these ADI schemes still require solution of a tridiagonal system of equations.

1.2 Present Work

A characteristic-based approach to spatial differencing has advantages in constructing implicit algorithms, as well as in utilizing the natural method of incorporating boundary conditions for hyperbolic systems. The ability of characteristic based methods to provide accurate nonreflecting solutions at outer boundaries is well known and is discussed for electromagnetics by Shang [10]–[11] and others.

The present method combines a characteristic based approach to spatial differencing with an implicit lower-upper approximate factorization (LU/AF) time integration scheme that can be developed as a two-factor scheme that retains its unconditional stability in three space dimensions, unlike three-factor ADI schemes. The LU/AF scheme also avoids the need to solve tridiagonal implicit systems. A two-factor approximate factorization for three dimensions was first suggested by Jameson and Turkel [25]. This type of factorization (two implicit passes in three dimensions) has been combined with characteristic based differencing by Belk and Whitfield [26]. This general approach has been further developed for CFD and is discussed, for example, in [27].

In the present report, an implicit characteristic based algorithm is developed for the time dependent Maxwell equations in one space dimension. This (one-dimensional) algorithm is investigated along two lines: A Fourier analysis is used to study both stability and dispersion/damping properties of the algorithm. Although the Fourier analysis provides useful information and is widely used to study algorithms, it is limited to periodic solutions on uniform grids. Complex practical applications often involve nonperiodic solutions in finite regions with complex geometry and nonuniform grids. Grid nonuniformity is an important consideration because conditional stability criteria typically link the maximum permissible time step to the local grid spacing rather

than to the underlying physical time and space "sampling" requirements of the solution. Stable implicit methods can benefit from choosing the time step to satisfy an accuracy requirement rather than a stability constraint, with the consequence that fewer time steps are needed for a fixed simulation time. Accordingly, a one-dimensional model problem with nonuniform grid is developed to explore the influence of grid nonuniformity on solution accuracy and efficiency. The explicit FDTD algorithm is used as a convenient reference algorithm for comparison.

In the remainder of this report, Section 2 develops first and second order, characteristic based, finite difference LU/AF algorithms for Maxwell's equations in one dimension. The second order scheme includes the conduction current term. Section 3 gives a Fourier analysis of stability, damping and dispersion properties of the one dimensional algorithms. Section 4 discusses the characteristic based treatment of boundary conditions. Section 5 gives computed model problem results related to both accuracy and efficiency for propagation and scattering in free space and dielectric materials, using both uniform and nonuniform grids. Finally, some conclusions are drawn in Section 6.

2 One-Dimensional LU/AF Algorithm

This section details the theoretical background for development of both first and second-order accurate LU/AF algorithms. The second order algorithm is used in all comparisons with the FDTD method, and the first order algorithm is used at points adjacent to the outer boundaries of the computational grid.

2.1 First-order algorithm

Maxwell's equations for linear, homogeneous and lossless media in the one-dimensional case (taking $\partial/\partial y = \partial/\partial z = 0$) are

$$\frac{\partial E_y}{\partial t} + \frac{1}{\epsilon}\frac{\partial H_z}{\partial x} = 0 \tag{1}$$

$$\frac{\partial H_z}{\partial t} + \frac{1}{\mu}\frac{\partial E_y}{\partial x} = 0 \tag{2}$$

These equations can be rewritten in flux conservative form as

$$\frac{\partial \bar{q}}{\partial t} + \frac{\partial \bar{f}}{\partial x} = 0 \tag{3}$$

where $\bar{q} = [E_y\ ,\ H_z]^T$, $\bar{f} = [H_z/\epsilon\ ,\ E_y/\mu]^T$ and T denotes transpose. To develop the upwind LU/AF algorithm, the flux conservative form of Maxwell's equations in (3) is recast in the following form

$$\frac{\partial \bar{q}}{\partial t} + \bar{A}\frac{\partial \bar{q}}{\partial x} = 0 \tag{4}$$

where $\bar{A}$ is the Jacobian of $\bar{f}$ and is given by

$$\bar{A} = \frac{\partial \bar{f}}{\partial \bar{q}} = \begin{bmatrix} 0 & 1/\epsilon \\ 1/\mu & 0 \end{bmatrix} \tag{5}$$

The matrix $\bar{A}$ has eigenvalues $\lambda_{1,2} = \pm 1/\sqrt{\mu\epsilon}$ corresponding to right and left propagating waves with speeds $\pm c$. The eigenvalue matrix is given by

$$\bar{\Lambda} = \begin{bmatrix} \lambda_1 & 0 \\ 0 & \lambda_2 \end{bmatrix} \tag{6}$$

The matrix $\bar{A}$ can be obtained from the eigenvalue matrix via a similarity transformation given by

$$\bar{A} = \bar{S}\bar{\Lambda}\bar{S}^{-1} \tag{7}$$

where the matrix $\bar{S}$ is composed of the eigenvectors of $\bar{A}$ and is given by

$$\bar{S} = \begin{bmatrix} \sqrt{\mu/\epsilon} & -\sqrt{\mu/\epsilon} \\ 1 & 1 \end{bmatrix}, \quad \bar{S}^{-1} = \frac{1}{2}\begin{bmatrix} \sqrt{\epsilon/\mu} & 1 \\ -\sqrt{\epsilon/\mu} & 1 \end{bmatrix} \tag{8}$$

The eigenvalue matrix $\bar{\Lambda}$ can be split into two parts, one each for the right and left propagating waves and is given by

$$\bar{\Lambda} = \bar{\Lambda}^+ + \bar{\Lambda}^- \tag{9}$$

$$\bar{\Lambda}^+ = \begin{bmatrix} \lambda_1 & 0 \\ 0 & 0 \end{bmatrix}, \quad \bar{\Lambda}^- = \begin{bmatrix} 0 & 0 \\ 0 & \lambda_2 \end{bmatrix} \tag{10}$$

Substituting (9) into (7) gives

$$\bar{A} = \bar{S}\left(\bar{\Lambda}^+ + \bar{\Lambda}^-\right)\bar{S}^{-1} = \bar{A}^+ + \bar{A}^- \tag{11}$$

$$\bar{A}^\pm = \bar{S}\bar{\Lambda}^\pm\bar{S}^{-1} \tag{12}$$

The flux vector $\bar{f}$ is then split into two parts given by

$$\bar{f} = \bar{f}^+ + \bar{f}^- \tag{13}$$

$$\bar{f}^\pm = \bar{A}^\pm\bar{q} \tag{14}$$

This flux-vector-splitting method is similar to that developed by Steger and Warming [28] for the Euler equations governing inviscid fluid flow. To construct the LU/AF algorithm, time and space are discretized to $t^n = n\Delta t$, $x_i = i\Delta x$ and the term $\partial\bar{f}/\partial x$ is approximated at $t = t^n + \beta\Delta t$ by

$$\frac{\partial\bar{f}}{\partial x} \approx \beta\left(\frac{\bar{f}_i^+ - \bar{f}_{i-1}^+}{\Delta x} + \frac{\bar{f}_{i+1}^- - \bar{f}_i^-}{\Delta x}\right)^{n+1} + (1-\beta)\left(\frac{\bar{f}_i^+ - \bar{f}_{i-1}^+}{\Delta x} + \frac{\bar{f}_{i+1}^- - \bar{f}_i^-}{\Delta x}\right)^{n} \tag{15}$$

Here, β $(0 \le \beta \le 1)$ is a parameter for evaluating the spatial approximation at $t^n + \beta\Delta t$. This will give an explicit scheme for $\beta = 0$ and an implicit scheme for $\beta > 0$. The finite difference equation for (3) is given by

$$\frac{\bar{q}_i^{n+1} - \bar{q}_i^n}{\Delta t} + \beta\left(\frac{\bar{f}_i^+ - \bar{f}_{i-1}^+}{\Delta x} + \frac{\bar{f}_{i+1}^- - \bar{f}_i^-}{\Delta x}\right)^{n+1} + (1-\beta)\left(\frac{\bar{f}_i^+ - \bar{f}_{i-1}^+}{\Delta x} + \frac{\bar{f}_{i+1}^- - \bar{f}_i^-}{\Delta x}\right)^{n} = 0 \tag{16}$$

Making the substitution $\Delta\bar{q}_i^n \equiv \bar{q}_i^{n+1} - \bar{q}_i^n$, equation (16) can be rearranged for a uniform grid to give

$$\left[\bar{I}/\Delta t + \beta\left(\Delta_{1i}^-\left(\bar{A}^+\cdot\right) + \Delta_{1i}^+\left(\bar{A}^-\cdot\right)\right)\right]\Delta\bar{q}_i^n = -\bar{R}_{1i}^n \tag{17}$$

where $\bar{I}$ is the 2 by 2 identity matrix, and

$$\Delta_{1i}^{-}(\cdot) \equiv \frac{(\cdot)_i - (\cdot)_{i-1}}{\Delta x} \tag{18}$$

$$\Delta_{1i}^{+}(\cdot) \equiv \frac{(\cdot)_{i+1} - (\cdot)_i}{\Delta x} \tag{19}$$

are the first-order backward and forward difference operators, respectively. The term $\bar{R}_{1i}^n$ is called the "residual" and is defined by

$$\bar{R}_{1i}^n \equiv \Delta_{1i}^{-} \bar{f}_i^{+,n} + \Delta_{1i}^{+} \bar{f}_i^{-,n} \tag{20}$$

Note that equation (17) is an *unfactored*, implicit scheme of $O\left[\Delta x, (\beta - 1/2)\,\Delta t, \Delta t^2\right]$ accuracy for the numerical solution of Maxwell's equations. The solution of (17) involves solving a block tridiagonal system of equations. The solution of tridiagonal systems can be avoided by an approximate factorization (AF) of the left side of (17) which results in the following LU/AF algorithm:

$$\left[\bar{I}/\Delta t + \beta \Delta_{1i}^{-}\left(\bar{A}^{+}\cdot\right)\right] \Delta \bar{q}_i^{*} = -\bar{R}_{1i}^n \tag{21}$$

$$\left[\bar{I}/\Delta t + \beta \Delta_{1i}^{+}\left(\bar{A}^{-}\cdot\right)\right] \Delta \bar{q}_i^{n} = \bar{I}/\Delta t \Delta \bar{q}_i^{*} \tag{22}$$

where Δq_i^* is an intermediate solution vector. This LU/AF algorithm is closely related to those developed previously for Computational Fluid Dynamics (e.g. [27]). It can be shown that these equations are a consistent and unconditionally stable approximation to (3), but the details of that analysis are omitted here for the sake of brevity. Note that the solution involves a two-step procedure. In solving (21), a sweep through the grid in the forward direction results in a block lower bidiagonal matrix and a sweep through the grid in the backward direction results in a block upper bidiagonal matrix for (22). These equations are then solved by forward and backward substitution, respectively. Thus, a costly inversion of a block tridiagonal matrix is avoided, and each step in the solution is effectively explicit. Substituting equation (22) into (21) and expanding gives,

$$\left[\bar{I}/\Delta t + \beta\left(\Delta_{1i}^{-}\left(\bar{A}^{+}\cdot\right) + \Delta_{1i}^{+}\left(\bar{A}^{-}\cdot\right)\right) + \beta^2 \Delta t\left(\Delta_{1i}^{-}\left(\bar{A}^{+}\cdot\right)\Delta_{1i}^{+}\left(\bar{A}^{-}\cdot\right)\right)\right] \Delta \bar{q}_i^{n} = -\bar{R}_{1i}^n \tag{23}$$

Note that equation (17) is recovered except for the third term in brackets, which represents the factorization error. In this particular example, $\bar{A}^{+}$ and $\bar{A}^{-}$ are constant matrices such that $\bar{A}^{+}\bar{A}^{-} \equiv 0$, and the factorization error is zero. However, the factorization error is nonzero in the following example with conduction currents, and more generally in two and three dimensional implementations. This error can be reduced or eliminated by iterative error reduction. The present one-dimensional model problem results do not include factorization error except for the case including conduction currents.

2.2 Second-order algorithm

To develop the $O\left(\Delta t^2, \Delta x^2\right)$ LU/AF algorithm, the flux conservative form of (4) is rewritten to include the electric and magnetic conduction currents as

$$\frac{\partial \bar{q}}{\partial t} + \bar{A}\frac{\partial \bar{q}}{\partial x} = -\bar{P}\,\bar{q} \tag{24}$$

where $\bar{P}$ is given by

$$\bar{P} = \begin{bmatrix} \sigma/\epsilon & 0 \\ 0 & \sigma^*/\mu \end{bmatrix} \tag{25}$$

and $\bar{A}$ is given by equation (5). The time derivative in (24) is approximated by a β-weighted, $O(\Delta t^2)$ difference equation given by

$$\frac{\partial \bar{q}}{\partial t} \approx \frac{(2\beta+1)q_i^{n+1} - 4\beta q_i^n + (2\beta-1)q_i^{n-1}}{2\Delta t} \tag{26}$$

The spatial derivative is again replaced by a β-weighted average between time level $n+1$ and n as in (15). This can be rewritten using the operator notation as

$$\frac{\partial \bar{f}}{\partial x} \approx \beta \left(\Delta_{2i}^- \bar{f}_i^+ + \Delta_{2i}^+ \bar{f}_i^-\right)^{n+1} + (1-\beta)\left(\Delta_{2i}^- \bar{f}_i^+ + \Delta_{2i}^+ \bar{f}_i^-\right)^n \tag{27}$$

The $\Delta_{2i}^{\pm}$ operators are now $O(\Delta x^2)$ difference operators to be defined shortly. The parameter β can be used to construct a series of explicit and implicit schemes. For example, if $\beta = 0$, this results in a leapfrog scheme; $\beta = 0.5$ results in a Crank-Nicolson scheme and $\beta = 1$ results in an Euler implicit scheme. Using (26) and (27), the finite-difference equation for (24) is

$$\frac{(2\beta+1)\Delta q_i^n - (2\beta-1)\Delta q_i^{n-1}}{2\Delta t} + \beta\left(\Delta_{2i}^- \bar{f}_i^+ + \Delta_{2i}^+ \bar{f}_i^-\right)^{n+1} + (1-\beta)\left(\Delta_{2i}^- \bar{f}_i^+ + \Delta_{2i}^+ \bar{f}_i^-\right)^n =$$
$$-\beta \bar{P}\,\bar{q}_i^{n+1} - (1-\beta)\bar{P}\bar{q}_i^n \tag{28}$$

Using the same flux vector splitting as in (14), this can be rearranged as

$$\left[\bar{I}/(2\Delta t) + \beta\alpha\bar{P} + \beta\alpha\left(\Delta_{2i}^- A^+(\cdot) + \Delta_{2i}^+ A^-(\cdot)\right)\right]\Delta\bar{q}_i^n = -\bar{R}_{2i}^n \tag{29}$$

The residual, $\bar{R}_{2i}^n$, is now defined by

$$\bar{R}_{2i}^n \equiv \alpha\left\{\bar{P}\bar{q}_i^n + \Delta_{2i}^- \bar{f}_i^{+,n} + \Delta_{2i}^+ \bar{f}_i^{-,n} - \frac{2\beta-1}{2\Delta t}\Delta\bar{q}_i^{n-1}\right\} \tag{30}$$

where $\alpha \equiv 1/(2\beta+1)$. The difference operators in equation (30) are replaced by $O(\Delta x^2)$ backward and forward upwind difference operators on three-point one-sided stencils defined by

$$\Delta_{2i}^-(\cdot) \equiv (3(\cdot)_i - 4(\cdot)_{i-1} + (\cdot)_{i-2})/(2\Delta x) \tag{31}$$
$$\Delta_{2i}^+(\cdot) \equiv (-3(\cdot)_i + 4(\cdot)_{i+1} - (\cdot)_{i+2})/(2\Delta x) \tag{32}$$

Substituting (14) into (30), the residual is given by

$$\bar{R}_{2i}^n = \alpha\left\{\bar{P}\bar{q}_i^n + \Delta_{2i}^- \bar{A}^+\bar{q}_i^n + \Delta_{2i}^+ \bar{A}^-\bar{q}_i^n - \frac{2\beta-1}{2\Delta t}\Delta\bar{q}_i^{n-1}\right\} \tag{33}$$

Equation (29) is an $O(\Delta t^2, \Delta x^2)$, unfactored, upwind scheme for electromagnetics. The LU/AF scheme is defined by factoring the left side of (29) into two operators, each designed for a forward and backward grid sweep as in the first order implementation. The LU/AF scheme is then given by

$$\left[\bar{I}/(2\Delta t) + \beta\alpha\bar{P} + \beta\alpha\Delta_{2i}^- \bar{A}^+(\cdot)\right]\Delta\bar{q}_i^* = -\bar{R}_{2i}^n \tag{34}$$
$$\left[\bar{I}/(2\Delta t) + \beta\alpha\bar{P} + \beta\alpha\Delta_{2i}^+ \bar{A}^-(\cdot)\right]\Delta\bar{q}_i^n = \left[\bar{I}/(2\Delta t) + \beta\alpha\bar{P}\right]\Delta\bar{q}_i^* \tag{35}$$

3 Fourier Analysis

A Fourier analysis shows that both the first and second-order upwind LU/AF algorithms are unconditionally stable for $\beta \geq 1/2$, and that they contain both numerical dissipation (or damping) and dispersion. The dissipation is present due to even order spatial derivatives in the truncation error which are a result of the upwind approximation. These schemes are consistent approximations with $O((\beta - 1/2)\Delta t, \Delta t^2, \Delta x)$ truncation error for the first-order algorithm and $O(\Delta t^2, \Delta x^2)$ for the second-order algorithm. A Fourier analysis is now given for the first-order LU/AF algorithm; the second-order algorithm analysis follows a similar development.

Assuming an equally spaced mesh with periodic boundary conditions, a trial solution of the form

$$\bar{q}_i^n = \bar{q}_0 e^{j(n\phi - i\theta)} \tag{36}$$

is substituted into equations (21) and (22) to obtain:

$$\bar{T}\,\Delta\bar{q}_i^n = \bar{U}\bar{q}_i^n \tag{37}$$

The matrices $\bar{T}$ and $\bar{U}$ are given by

$$\bar{T} = \left[\bar{I} + \frac{\beta\nu}{c}\left(1 - e^{j\theta}\right)\bar{A}^+\right]\left[\bar{I} + \frac{\beta\nu}{c}\left(e^{-j\theta} - 1\right)\bar{A}^-\right] \tag{38}$$

$$\bar{U} = -\left(\frac{\nu}{c}\left(1 - e^{j\theta}\right)\bar{A}^+ + \frac{\nu}{c}\left(e^{-j\theta} - 1\right)\bar{A}^-\right) \tag{39}$$

where $c = 1/\sqrt{\mu\epsilon}$, ν is the Courant number defined by $\nu = c\Delta t/\Delta x$ and $\phi = \nu\theta$. Again making the substitution $\Delta\bar{q}_i^n \equiv \bar{q}_i^{n+1} - \bar{q}_i^n$, equation (37) can be rearranged to give

$$\bar{q}_i^{n+1} = \bar{G}\bar{q}_i^n \tag{40}$$

where the amplification matrix $\bar{G}$ is defined by

$$\bar{G} = \bar{I} + \bar{T}^{-1}\bar{U} \tag{41}$$

The stability of this scheme is governed by the spectral radius of the amplification matrix $\bar{G}$, and its eigenvalues, G_1 and G_2. Closed form solutions were obtained for G_1 and G_2, but they are omitted here for the sake of brevity. A rigorous numerical stability analysis was also performed on the second-order LU/AF algorithm using the $MAPLE\ 6^{TM}$ software package. Checking the magnitude of the eigenvalues G_1 and G_2 for all values of β, ν and θ showed that both the first and second-order schemes are unconditionally stable for $\beta \geq 1/2$. The stability analysis in this particular case is identical to the unfactored implicit scheme given in equation (17), because the factorization error is zero for $\bar{P} = 0$.

For the dispersion analysis, the term

$$\bar{q}_i^{n+1} = \bar{q}_i^n\, e^{j\phi^*} \tag{42}$$

is substituted in (40) to give

$$\left(\bar{G} - e^{j\phi^*}\bar{I}\right)\bar{q}_i^n = 0 \tag{43}$$

Equation (43) is then solved for ϕ^*, the numerical wavenumber. The quantity $\Im m\{\phi^*/\phi\}$ gives the numerical dispersion, or phase velocity error. Extensive numerical experiments were performed to analyze the dispersive properties of these algorithms. We let $\theta = 2\pi/N$, where N is the grid resolution in cells/λ. Figure 1 shows the numerical dispersion versus grid resolution with $\nu = 3/4$ for the first and second-order LU/AF algorithms as compared to the FDTD algorithm, which is $O(\Delta t^2, \Delta x^2)$. The Courant number of $\nu = 3/4$ was chosen for these methods simply as a representative Courant number which could be expected for a problem involving a nonuniform grid. For a nonuniform mesh with a mesh stretch ratio of $M_s : 1$ where $M_s \equiv \Delta x_{max}/\Delta x_{min}$, the Courant number for FDTD varies pointwise in the grid over the range $1/M_s \leq \nu_i \leq 1$, where $\nu_i \equiv (c\Delta t)/\Delta x_i$. The numerical experiments showed that the first-order LU/AF algorithm has

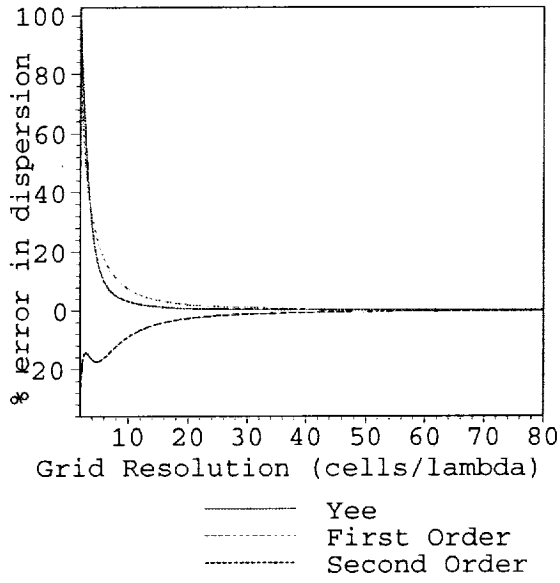

Figure 1: Numerical dispersion of FDTD, first and second-order LU/AF algorithms versus grid resolution for $\beta = 1/2$ and $\nu = 3/4$.

lower dispersion errors than the second-order LU/AF method for $\nu \leq 1$. This is not particularly troublesome, because for $\nu \leq 1$, explicit schemes are generally more efficient and are preferred. However, for $\nu > 1$, explicit schemes cannot be used and the second-order LU/AF algorithm does have lower dispersion error than the first-order LU/AF method. For large values of ν, the dispersive error for the first and second-order LU/AF schemes begin to converge as shown in Figure 2. The results also showed that the lowest numerical dispersion is obtained when $\beta = 1/2$ as shown in Figure 3. Since the LU/AF method uses windward differencing, numerical dissipation (or damping) is present in the solution. The normalized dissipation is obtained as $\Re e\{\phi^*/\phi\}$. Figures 4-6 show numerical dissipation for the first and second-order LU/AF schemes versus grid resolution, ν and β, respectively. Note that the second-order algorithm has much lower dissipation than the first order method.

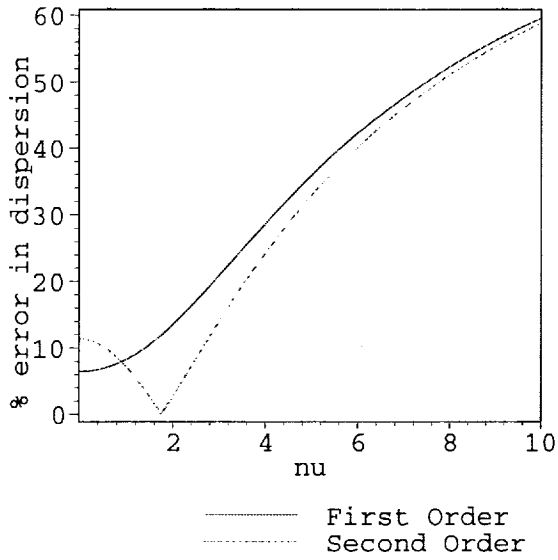

Figure 2: Numerical dispersion of first and second-order LU/AF algorithms versus Courant number ν at $\beta = 1/2$ and $N = 10$ cells/λ resolution.

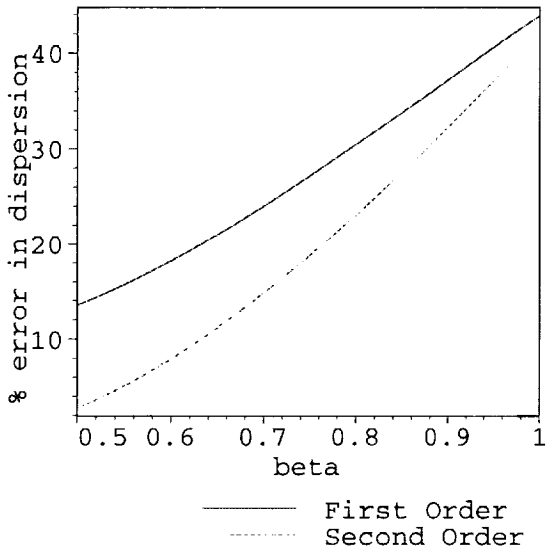

Figure 3: Numerical dispersion of first and second-order LU/AF algorithms versus β at $\nu = 2$ and $N = 10$ cells/λ resolution.

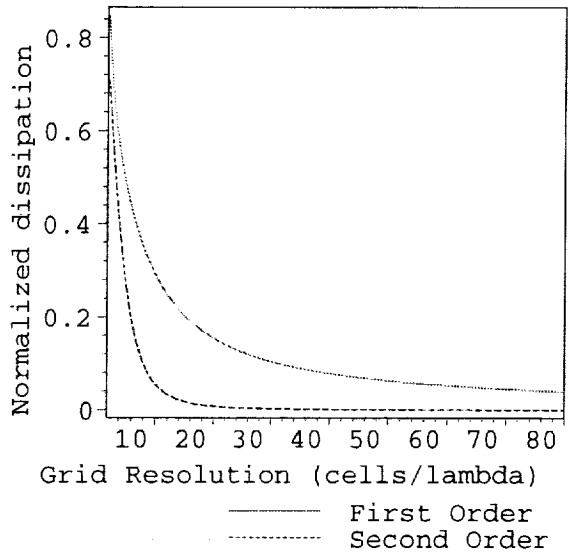

Figure 4: Normalized dissipation of first and second-order LU/AF algorithms versus grid resolution at $\beta = 0.5$ and $\nu = 0.75$.

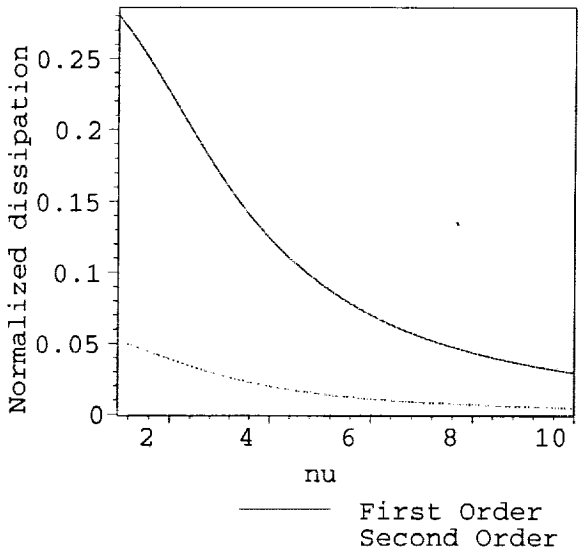

Figure 5: Normalized dissipation of first and second-order LU/AF algorithms versus Courant number ν at $\beta = 1/2$ and $N = 10$ cells/λ resolution.

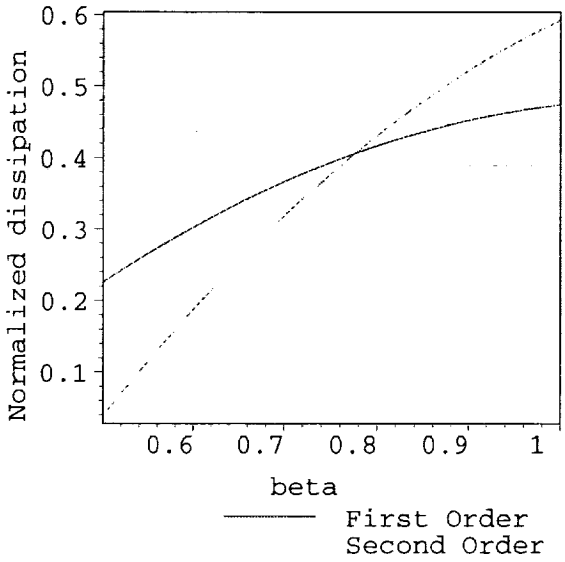

Figure 6: Normalized dissipation of first and second-order LU/AF algorithms versus β at $\nu = 2$ and $N = 10$ cells/λ resolution.

4 Boundary Conditions

4.1 Outer Radiation Boundary Condition

The characteristic based LU/AF method requires no extraneous boundary condition such as the Liao absorbing boundary condition [29] or the PML [30]. The FDTD method uses a spatial central difference operator, which for a wave propagating from left to right, eventually requires a grid point *outside* the domain. This requirement introduces an additional equation (i.e. boundary condition) to solve the system and introduces information into the solution that is not required by Maxwell's equations. Using an upwind characteristic based approach, the interior point algorithm calculates the left-going characteristic at the left boundary (i.e. at $i = 0$) and the right-going characteristic at the right boundary (i.e. at $i = imax$). Therefore, the only additional information required is information about waves that are *entering* the domain. Waves exiting the domain are naturally handled by the interior point algorithm. Therefore, the characteristic boundary conditions are implemented as follows: at grid point $i = 0$, equation (22) is used along with a specification of the incoming, right-going flux, f_0^+. At grid point $i = imax$, equation (21) is used along with a specification of the incoming, left-going flux, f_{imax}^-. Therefore, the only additional information introduced at the boundary is nothing more than what is required by the physical system. In multidimensional problems, the local coordinates at the outer boundaries are rotated to align with the direction of wave propagation defined by $\bar{E} \times \bar{H}$. The characteristic equations are developed along this direction and are appropriately applied at the boundaries. This procedure was discussed and outlined by Shang [11].

4.2 Dielectric Surface Boundary Condition

Since the LU/AF scheme follows the direction of information propagation (i.e. the *characteristic*), at a material interface, the slope of the characteristic curve (i.e. the speed of light in the material) changes. Therefore, for the LU/AF method to be widely applicable, a careful treatment of material interfaces is required. With a material boundary in place, the right-going and left-going characteristics see a change in characteristic speeds, and therefore, a material interface condition needs to be implemented to correctly model the physics. To implement this feature, consider the one-dimensional grid shown in Figure 7 where a dielectric boundary has been inserted at grid point i_b. For the second order LU/AF method, at an arbitrary grid point i, the windward differ-

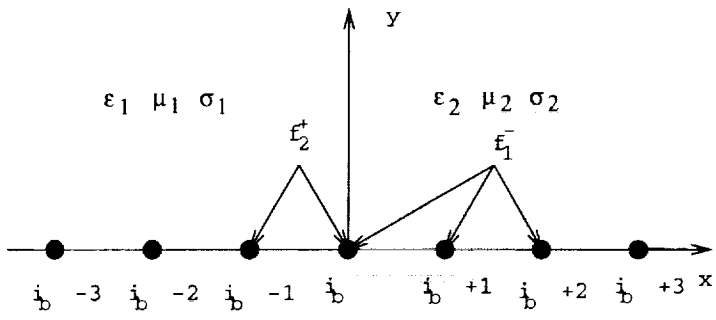

Figure 7: One-dimensional FDTD grid showing a dielectric boundary at grid point i_b.

encing uses flux components f^+_{i-2}, f^+_{i-1}, f^+_i, f^-_i, f^-_{i+1}, f^-_{i+2}. This creates a difficulty at a dielectric interface since the algorithm assumes the material is homogeneous. We know at grid point i_b that the physical boundary conditions require that

$$E_{tan1} = E_{tan2} \tag{44}$$
$$H_{tan1} = H_{tan2} \tag{45}$$

which requires that

$$E_{y1} = E_{y2} \tag{46}$$
$$H_{z1} = H_{z2} \tag{47}$$

Imposing these boundary conditions at i_b then makes the solution vector $\bar{q}$ constant between material 1 and 2. Therefore, the same solution vector $\bar{q}$ can be used for both materials at grid point

i_b. In general, in regions 1 and 2, we require flux components f_1^+, f_1^-, f_2^+ and f_2^-, which are restricted to the respective materials and are dependent on the material properties. However, we define *additional* flux components f_1^- located at grid points i_b, $i_b + 1$ and $i_b + 2$ in material 2 and flux components f_2^+ at grid points i_b and $i_b - 1$ in material 1. By defining these components, we can then apply the second order windward difference formulas at grid points $i_b - 2$, $i_b - 1$, i_b, $i_b + 1$ and $i_b + 2$ to *simulate* a homogeneous material region. For example, on the forward sweep, at grid point i_b, we use the components $f_1^+(i_b - 2)$, $f_1^+(i_b - 1)$, $f_1^+(i_b)$, $f_1^-(i_b)$, $f_1^-(i_b + 1)$, $f_1^-(i_b + 2)$ to update the solution vector $\bar{q}$ using the material properties of region 1. Similar analogies can be drawn at grid points $i_b - 2$, $i_b - 1$, $i_b + 1$ and $i_b + 2$. These additional fluxes in each region in the vicinity of the dielectric boundary are computed from (14) based upon the material properties in each region, and they bridge the solution between regions 1 and 2.

5 Model Problem Results

The model problem results presented in this section demonstrate that the one dimensional implicit characteristic-based LU/AF algorithm can produce accurate results on a nonuniform grid for time steps significantly larger than the maximum permissible for a typical conditionally stable scheme. Although the operation count for the implicit scheme is higher, as the mesh variation is increased, fewer time steps are needed for an accurate solution over a fixed simulation time, and this savings more than offsets the additional operations (beyond a certain mesh variation).

The second-order LU/AF algorithm was tested by implementing equations (34) and (35) for interior grid points away from absorbing boundaries and equations (21), (22) at grid points next to the absorbing boundaries. Characteristic-based boundary conditions were used to terminate the computational domain and the incoming flux (f_{imax}^-) at the right boundary was set to zero. The code was initialized by writing a time snapshot of a propagating pulse in the grid. Several different types of problems were analyzed with the LU/AF algorithm and compared with the FDTD method in an attempt to assess the characteristics of the LU/AF algorithm as applied to a one-dimensional problem with a non-uniform grid. These are outlined in the following sections.

5.1 Propagation

To assess the dispersion and dissipation characteristics of the LU/AF algorithm, several propagation problems were analyzed using free space and dielectric materials and were compared with FDTD. A Gaussian pulse of the form

$$E_{yi} = e^{-\left(\frac{(t-t_0)}{\tau}\right)^2} \tag{48}$$

was used as an excitation source for both propagation and scattering problems. For propagation, the code was changed to use periodic boundary conditions to enable simulation of propagation over large distances compared to the shortest wavelength contained in the frequency spectrum of the pulse. To illustrate the potential benefit of the LU/AF algorithm over conventional explicit schemes, the main parameters of interest are the time resolution (i.e. number of time steps/period) and the grid resolution (i.e. number of cells/wavelength) of the highest frequency of interest in

any given problem. These parameters will be designated as N_t and N_x, respectively. The other parameter of interest is the mesh stretch ratio, M_s. The highest frequency of interest, f_{max}, is calculated based upon N_x and the largest cell size, and the time step for the implicit scheme is calculated based upon f_{max} and the desired time resolution, N_t. For the FDTD method, the time step was calculated based upon the Courant stability condition using the smallest grid size.

The first propagation problem involves propagation in free space on a uniform mesh. The time and grid resolutions are $N_t = 30$ and $N_x = 30$, the cell size was 1 cm, the time step was 33.3 ps and $\nu = 1$. The maximum frequency of interest was 1 GHz and the problem space was 2000 cells. The pulse was allowed to propagate a distance equal to 100 wavelengths of the minimum wavelength, which corresponds to a distance of about 30 meters. Figure 8 shows the electric field versus distance obtained after 3000 time steps computed using the exact solution, FDTD and the LU/AF algorithm. Note the LU/AF scheme has slightly less accurate results due to the larger dis-

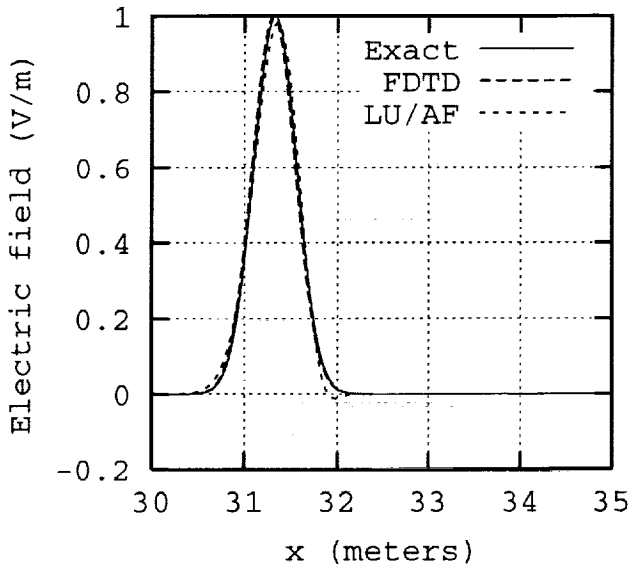

Figure 8: Electric field versus distance for free space propagation on a uniform mesh with $\beta = 1/2$ and $\nu = 3/4$.

persion error; but the general shape of the pulse is still acceptable. Again, this is not troublesome, because for $\nu \leq 1$, explicit schemes are more efficient and are preferred. Further numerical simulations confirmed that the numerical dispersion was lower and the results were more accurate for the second-order LU/AF method for the case when $\nu = 2$ as shown in Figure 9. Additional simulations confirmed that the numerical dispersion error increases with Courant number ν as with the ADI FDTD scheme [24].

To demonstrate the LU/AF scheme on nonuniform meshes, the same problem outlined above was simulated using mesh stretch ratios of M_s=10:1 and M_s=100:1 and the mesh was periodic every 10 cells. Figure 10 illustrates an expanded section of the nonuniform mesh for a mesh stretch ratio of M_s =10:1. The smallest grid cells force the FDTD algorithm to take a time step 1/10th of the previous case, and it must run 10 times as many time steps to propagate the pulse the same

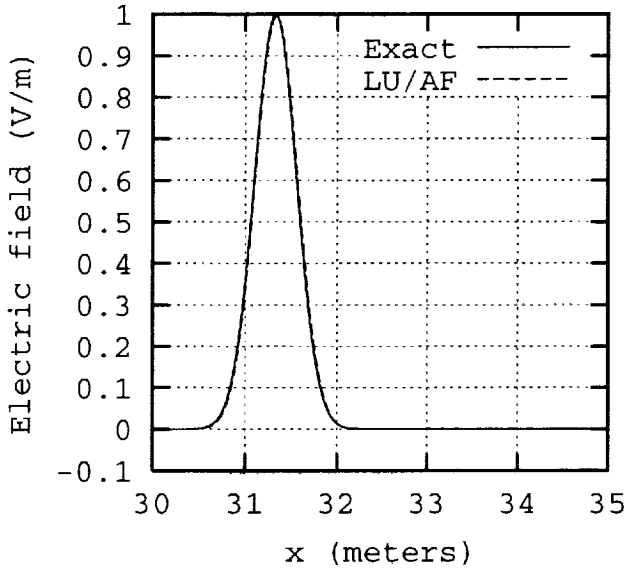

Figure 9: Electric field versus distance for free space propagation on a uniform mesh with $\beta = 1/2$ and $\nu = 2$.

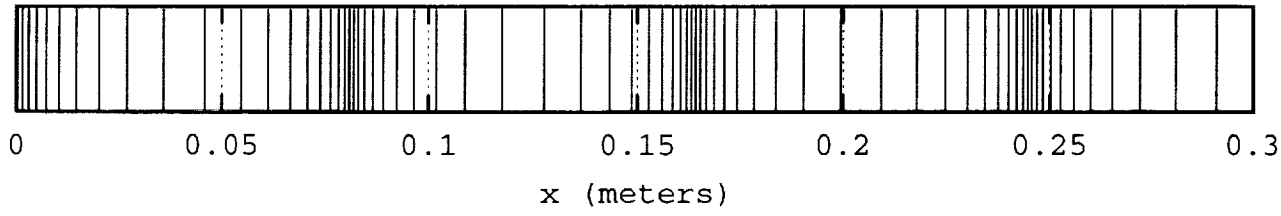

Figure 10: A section of a nonuniform mesh with a mesh stretch ratio of 10:1 and largest cell size of 1 cm.

distance. However, the LU/AF algorithm can take the same time step as before, because the time resolution, $N_t = 30$, has been preserved and the time step is set solely upon accuracy requirements, not on the Courant stability condition. The maximum cell size remains constant, and since N_x is also the same, the maximum frequency of interest remains constant at 1 GHz. The maximum grid coordinate changes from 20.0 m in the uniform mesh case to 8.17 m for the 10:1 nonuniform mesh. The Courant numbers in the grid for FDTD are in the range $0.1 \leq \nu \leq 1$ and the Courant numbers for the LU/AF algorithm are in the range $1 \leq \nu \leq 10$. Figure 11 shows the electric field versus distance obtained with the exact solution and after 30,000 time steps computed using FDTD and after 3,000 time steps using the LU/AF algorithm. Note the agreement is very good

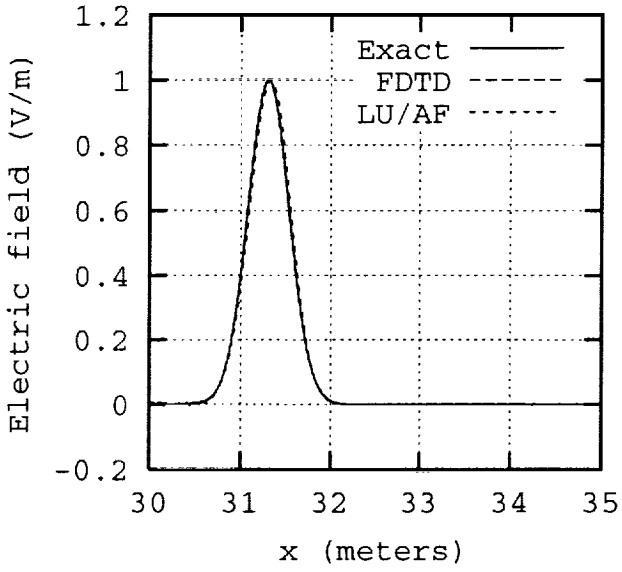

Figure 11: Electric field versus distance for free space propagation on a nonuniform mesh with $\beta = 1/2$ and $\nu = 1$.

for both methods in this case. In fact, Figure 12 shows the error in electric field versus distance for both methods and the errors are almost equal in magnitude. The LU/AF method still required about 15 seconds, but the FDTD method required about 22 seconds. Note the improved performance of the LU/AF algorithm away from the area of the main pulse. Since the mesh stretch ratio was 10 for this problem, the FDTD method is forced by the Courant stability condition to take 10 times the number of time steps to simulate the same amount of physical time. It appears that the crossover point in efficiency between the LU/AF and FDTD methods is approximately a mesh stretch ratio of 10:1. This is in contrast to recent results for the ADI FDTD scheme [23] where the results suggested a crossover point of 30:1 mesh ratio.

For a mesh stretch ratio of M_s =100:1, the Courant number for FDTD was in the range $0.01 \leq \nu \leq 1$ and for LU/AF was in the range $1 \leq \nu \leq 100$. Execution time for FDTD was 230 seconds for 300,000 time steps. Execution time for the LU/AF method again required 15 seconds for 3,000 times steps and the error in electric field for this simulation is shown in Figure 13. Note again that the LU/AF result appears "cleaner" than the FDTD result with less numerical noise. Based upon these results, we conclude that the LU/AF method is more efficient for *either* a.) nonuni-

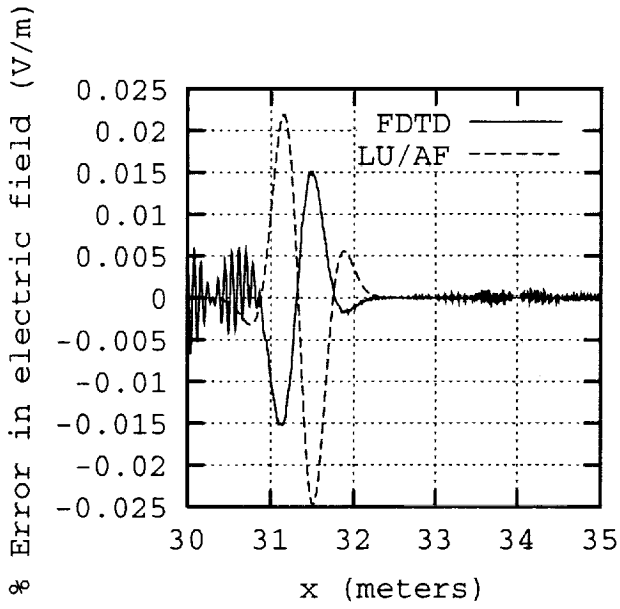

Figure 12: Error in electric field versus distance for free space propagation on a nonuniform mesh with a mesh stretch ratio of 10:1 and $\beta = 1/2$, $\nu = 1$ (for FDTD).

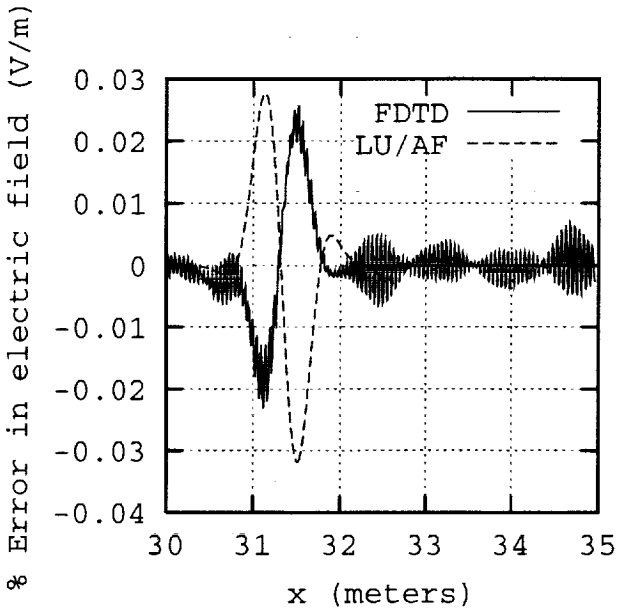

Figure 13: Error in electric field versus distance for free space propagation on a nonuniform mesh with a mesh stretch ratio of 100:1 and $\beta = 1/2$, $\nu = 1$ (for FDTD).

form meshes with large mesh stretch ratios *or* b.) a uniform mesh with a low frequency incident excitation, where the pulse is highly resolved spatially over its entire frequency spectrum. Further computational experience on additional free space propagation problems on nonuniform grids reveals that this sweeping method fails for large Δt (i.e. large Courant number). This can occur for two reasons, even though the Fourier stability analysis indicates unconditional stability. First, it is inapropriate to use a time step larger than one which propagates a wave over a distance comparable to the entire solution domain in a single time step, and this can cause instability. Secondly, the spatial sweeping process associated with each factor of the algorithm can itself become unstable if it loses diagonal dominance, as observed by Jameson and Turkel [25]. Although a first-order spatial upwind scheme guarantees diagonal dominance, there is a loss of diagonal dominance for higher-order upwind schemes as the time step becomes asymptotically large. The upwind scheme significantly increases the diagonal term compared with a centered scheme, however, and in applying the LU/AF scheme, this problem can be avoided by exercising care in selecting the time step.

5.2 Lossy Dielectric Materials

To illustrate propagation in dielectric materials, the problem space was filled with a lossy dielectric material with parameters $\epsilon = 4\epsilon_0$, $\mu = \mu_0$ and $\sigma = 0.02$. The pulse was allowed to propagate on a uniform mesh for approximately 35 wavelengths at the minimum wavelength. Figure 14 shows the results of FDTD versus LU/AF with excellent agreement between the two methods. A similar level of agreement is found with the same problem on a nonuniform grid.

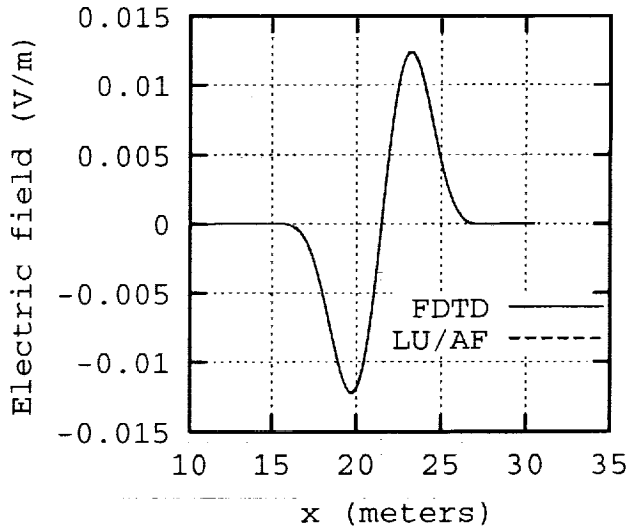

Figure 14: Electric field versus distance for propagation in a lossy dielectric on a uniform mesh with $\beta = 1/2$ and $\nu = 1$.

To illustrate the use of the LU/AF scheme for scattering problems, reflection from a lossy dielectric half-space was considered as the benchmark problem. The dielectric interface scheme

of Section 4.2 was implemented and the results are again compared with the FDTD method. To solve this problem, the problem space is 2000 cells and it is filled with a lossy dielectric material from cell numbers 751-2000. The total electric field is recorded versus time at cell number 750. The incident field is obtained by running the code with free space only and recording the field versus time at the same location. The incident field is subtracted from the total field to give the scattered field. A point source located at the left boundary of the grid was used as the excitation source and the dielectric half-space material parameters are $\epsilon = 4\epsilon_0$, $\mu = \mu_0$ and $\sigma = 0.2$ S/m. Figure 15 shows the time-domain scattered field for this case, and the agreement is excellent. Figure 16

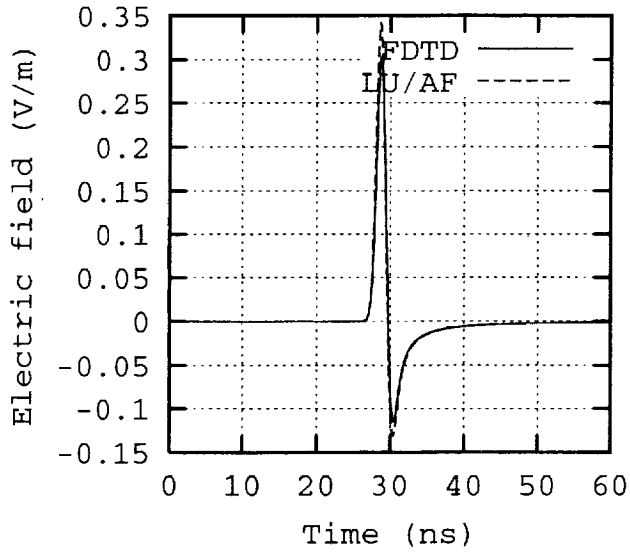

Figure 15: Scattered electric field versus time for scattering from a lossy dielectric half-space on a uniform mesh with $\beta = 1/2$ and $\nu = 1$.

shows the reflection coefficient results and again the agreement is excellent. The same problem was run on the uniform mesh with $\sigma = 2$, and on a nonuniform mesh with a mesh stretch ratio of 10:1 and $\sigma = 0.2$ S/m. Figures 17 and 18 show the respective results.

Note that the LU/AF method produces more inaccurate results for moderate conductivity values. This is due to the factorization error terms. As σ is increased, the factorization errors become larger. In principle, this factorization error can be reduced throught iterative error reduction [31]. This has been demonstrated for CFD problems [27], but it is not explored in the present work. For perfect conductors, we simply set $\bar{q} = 0$. Figure 18 shows that the LU/AF method is superior on nonuniform grids, even for problems involving lossy dielectrics. These results indicate that the physical dielectric boundary conditions have been properly implemented, thus making the LU/AF method applicable to a wider class of problems.

6 Conclusions

This report has introduced a LU/AF implicit finite-difference method for computational electromagnetics. A second-order accurate, LU/AF, characteristic based algorithm for electromag-

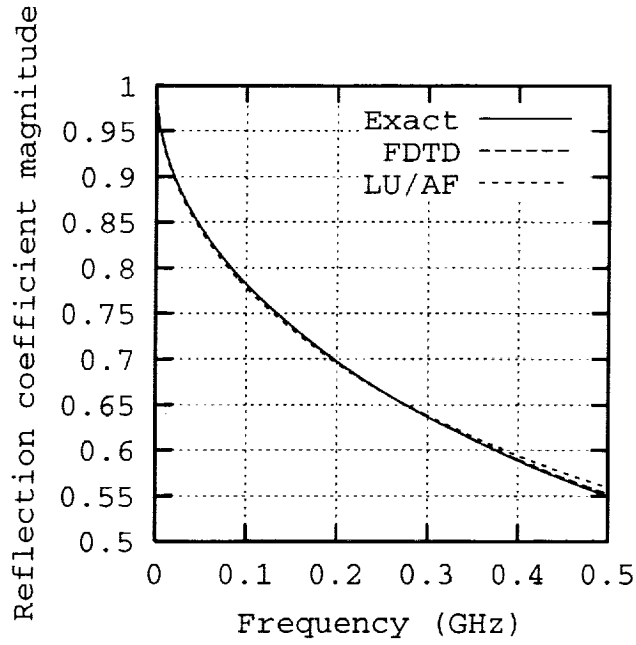

Figure 16: Reflection coefficient magnitude versus frequency for scattering from a lossy dielectric half-space on a uniform mesh with $\beta = 1/2$ and $\nu = 1$.

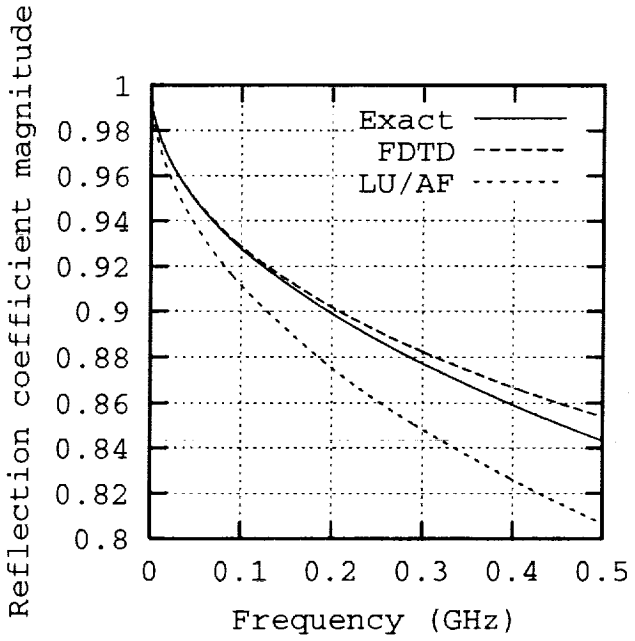

Figure 17: Reflection coefficient magnitude versus frequency for scattering from a lossy dielectric half-space on a uniform mesh with $\beta = 1/2$, $\nu = 1$ and $\sigma = 2$ S/m.

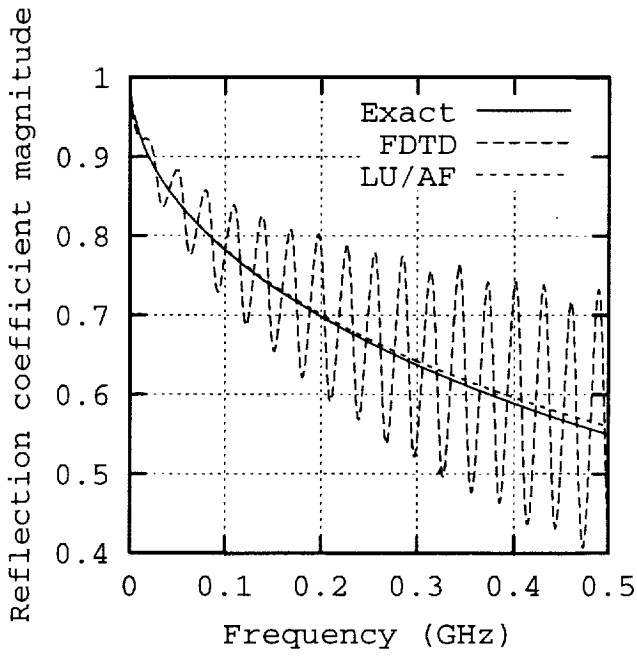

Figure 18: Reflection coefficient magnitude versus frequency for scattering from a lossy dielectric half-space on a uniform mesh with $\beta = 1/2$, $\nu = 1$ and $\sigma = 0.2$ S/m.

netics has been implemented and tested on one-dimensional model problems for uniform and nonuniform grids. The one-dimensional model problem results for the characteristic based implicit scheme demonstrate that:

1. Accurate solutions for wave propagation can be obtained using Courant number significantly greater than one on nonuniform grids.

2. Stability of the implicit scheme allows a given amount of time to be covered in fewer time steps than a conditionally stable scheme, and this can significantly improve efficiency when nonuniform grids are needed. This is also extremely beneficial for low frequency excitation sources where geometric details may force a highly oversampled mesh (uniform or nonuniform) in certain regions.

3. The method works well with lossy dielectric materials and perfect conductors.

4. The factorization error increases as σ increases, but it can be reduced in principle through iterative error reduction.

5. The lowest dispersion and damping errors occur when $\beta = 1/2$.

The present results demonstrate potential advantages in a one dimensional context, and this approach appears promising for development of stable, accurate and efficient implicit LU/AF schemes for complex two and three dimensional applications. Extensions to two and three-dimensional applications have been outlined [31], but details of this work will the subject of future reports and articles.

References

[1] K. S. Yee, "Numerical solution of initial boundary value problems involving Maxwell's equations in isotropic media," *IEEE Transactions on Antennas and Propagation*, vol. 14, no. 3, pp. 302–307, Mar. 1966.

[2] K. S. Kunz and R. J. Luebbers, *The Finite Difference Time Domain Method for Electromagnetics*, CRC Press, Boca Raton, FL, 1993.

[3] A. Taflove, *Computational Electrodynamics: The Finite-Difference Time-Domain Method*, Artech House, Boston, MA, 1995.

[4] A. Taflove, Ed., *Advances in Computational Electrodynamics: The Finite-Difference Time-Domain Method*, Artech House, Boston, MA, 1998.

[5] R. Holland, L. Simpson, and K. Kunz, "Finite-difference analysis of EMP coupling to lossy dielectric structures," *IEEE Transactions on Electromagnetic Compatibility*, vol. EMC-22, no. 3, pp. 203–209, Aug. 1980.

[6] R. F. Warming and R. M. Beam, "An extension of a-stability to alternating direction implicit methods," *BIT*, vol. 19, pp. 395–417, 1979.

[7] R. C. Buggeln W. R. Briley and H. McDonald, "Solution of the three-dimensional navier stokes equations for a steady laminar horseshoe vortex flow," in *Proc. 7th Computational Fluid Dynamics Conference*, Cincinnati, OH, July 1985, AIAA Paper 85-1520-CP.

[8] W. F. Hall V. Shankar and A. H. Mohammadian, "A time-domain differential solver for electromagnetic problems," *Proc. IEEE*, vol. 77, no. 5, pp. 709–721, May 1989.

[9] W. F. Hall V. Shankar and A. H. Mohammadian, "A time-domain, finite-volume treatment for the Maxwell equations," *Electromagnetics*, vol. 10, pp. 127, 1990.

[10] J. S. Shang, "Characteristic based methods for the time-domain Maxwell equations," in *AIAA 29th Aerospace Sciences Meeting & Exhibit*, Reno, NV, Jan. 1991, vol. AIAA 91-0606.

[11] J. S. Shang, "A characteristic-based algorithm for solving 3-d time-domain Maxwell equations," in *AIAA 30th Aerospace Sciences Meeting & Exhibit*, Reno, NV, Jan. 1992, vol. AIAA 92-0452.

[12] J. S. Shang, "A fractional-step method for solving 3-d time-domain Maxwell equations," in *AIAA 31st Aerospace Sciences Meeting & Exhibit*, Reno, NV, Jan. 1993, vol. AIAA 93-0461.

[13] J. S. Shang and D. Gaitonde, "Characteristic-based, time-dependent Maxwell equations solvers on a general curvilinear frame," in *AIAA 24th Plasmadynamics & Lasers Conference*, Orlando, FL, July 1993, vol. AIAA 93-3178.

[14] K. C. Hill J. S. Shang and D. Calahan, "Performance of a characteristic-based, 3-d time-domain Maxwell equations solvers on a massively parallel computer," in *AIAA 24th Plasmadynamics & Lasers Conference*, Orlando, FL, July 1993, vol. AIAA 93-3179.

[15] J. S. Shang and R. M. Fithen, "A comparative study of numerical algorithms for computational electromagnetics," in *AIAA 25th Plasmadynamics & Lasers Conference*, Colorado Springs, CO, June 1994, vol. AIAA 94-2410.

[16] J. S. Shang and D. Gaitonde, "Characteristic-based, time-dependent Maxwell equation solvers on a general curvilinear frame," *AIAA Journal*, vol. 33, no. 3, pp. 491–498, March 1995.

[17] J. S. Shang, "A fractional-step method for solving 3d, time-domain Maxwell equations," *Journal of Comp. Phys.*, vol. 118, pp. 109–119, 1995.

[18] J. S. Shang and R. M. Fithen, "A comparative study of characteristic-based algorithms for the Maxwell equations," *Journal of Comp. Phys.*, vol. 125, pp. 378–394, 1996.

[19] D. C. Blake and J. S. Shang, "A procedure for rapid prediction of electromagnetic scattering from complex objects," in *AIAA 29th Plasmadynamics & Lasers Conference*, Albuquerque, NM, June 1998, vol. AIAA 98-2925.

[20] D. Gaitonde and J. S. Shang, "High-order finite-volume schemes in wave propagation phenomena," in *AIAA 27th Plasmadynamics & Lasers Conference*, New Orleans, LA, June 1996, vol. AIAA 96-2335.

[21] F. Zheng, Z. Chen, and J. Zhang, "A finite-difference time-domain method without the Courant stability conditions," *IEEE Microwave Guided Wave Letters*, vol. 9, no. 11, pp. 441–443, Nov. 1999.

[22] F. Zheng, Z. Chen, and J. Zhang, "Toward the development of a three-dimensional unconditionally stable finite-difference time-domain method," *IEEE Transactions on Microwave Theory and Techniques*, vol. 48, no. 9, pp. 1550–1558, Sept. 2000.

[23] T. Namiki, "3-D ADI-FDTD method—Unconditionally stable time-domain algorithm for solving full vector Maxwell's equations," *IEEE Transactions on Microwave Theory and Techniques*, vol. 48, no. 10, pp. 1743–1748, Oct. 2000.

[24] A. Taflove and S. Hagness, *Computational Electrodynamics: The Finite-Difference Time-Domain Method, 2 ed.*, Artech House, Boston, MA, 2000.

[25] A. Jameson and E. Turkel, "Implicit schemes and approximate factorizations," *Math. Comp.*, vol. 37, pp. 385–397, 1981.

[26] D. M. Belk and D. L. Whitfield, "Unsteady three-dimesional euler solutions on blocked grids using an implicit two-pass algorithm," January 1987, vol. AIAA Paper No. 87-0450.

[27] W. R. Briley, S. S. Neerarambam, and D. L. Whitfield, "Implicit Lower-Upper/Approximate-Factorization algorithms for incompressible flows," *Journal of Comp. Phys.*, vol. 128, pp. 32–42, 1996.

[28] J. L. Steger and R. F. Warming, "Flux vector splitting of the invisid gas dynamic equations with applications to finite difference methods," *Journal of Comp. Phys.*, vol. 4, no. 2, pp. 263–293, 1981.

[29] Z. P. Liao, H. L. Wong, B.-P. Yang, and Y.-F. Yuan, "A transmitting boundary for transient wave analysis," *Sci. Sin., Ser. A*, vol. 27, no. 10, pp. 1063–1076, Oct. 1984.

[30] J.-P. Berenger, "A perfectly matched layer for the absorption of electromagnetic waves," *Journal of Computational Physics*, vol. 114, no. 1, pp. 185–200, 1994.

[31] J. H. Beggs and W. R. Briley, "An implicit characteristic based method for computational electromagnetics," Tech. Rep. MSSU-EIRS-ERC-98-11, Miss. State Univ., August 1998.

REPORT DOCUMENTATION PAGE

Form Approved
OMB No. 0704–0188

1. AGENCY USE ONLY *(Leave blank)*	2. REPORT DATE	3. REPORT TYPE AND DATES COVERED
	May 2001	Technical Memorandum

4. TITLE AND SUBTITLE
An Implicit Characteristic Based Method for Electromagnetics

5. FUNDING NUMBERS
706–31–41–01

6. AUTHOR(S)
John H. Beggs, W. Roger Briley

7. PERFORMING ORGANIZATION NAME(S) AND ADDRESS(ES)
NASA Langley Research Center
Hampton, VA 23681–2199

8. PERFORMING ORGANIZATION REPORT NUMBER
L–18051

9. SPONSORING/MONITORING AGENCY NAME(S) AND ADDRESS(ES)
National Aeronautics and Space Administration
Washington, DC 20546–0001

10. SPONSORING/MONITORING AGENCY REPORT NUMBER
NASA/TM–2001–210862

11. SUPPLEMENTARY NOTES

12a. DISTRIBUTION/AVAILABILITY STATEMENT
Unclassified-Unlimited
Subject Category 33 Distribution: Standard
Availability: NASA CASI (301) 621–0390

12b. DISTRIBUTION CODE

13. ABSTRACT ***(Maximum 200 words)***
An implicit characteristic-based approach for numerical solution of Maxwell's time-dependent curl equations in flux conservative form is introduced. This method combines a characteristic based finite difference spatial approximation with an implicit lower-upper approximate factorization (LU/AF) time integration scheme. This approach is advantageous for three-dimensional applications because the characteristic differencing enables a two-factor approximate factorization that retains its unconditional stability in three space dimensions, and it does not require solution of tridiagonal systems. Results are given both for a Fourier analysis of stability, damping and dispersion properties, and for one-dimensional model problems involving propagation and scattering for free space and dielectric materials using both uniform and nonuniform grids. The explicit FDTD algorithm is used as a convenient reference algorithm for comparison. The one-dimensional results indicate that for low frequency problems on a highly resolved uniform or nonuniform grid, this LU/AF algorithm can produce accurate solutions at Courant numbers significantly greater than one, with a corresponding improvement in efficiency for simulating a given period of time. This approach appears promising for development of dispersion optimized LU/AF schemes for three dimensional applications.

14. SUBJECT TERMS
computational electromagnetics, FDTD methods

15. NUMBER OF PAGES
29

16. PRICE CODE
A03

17. SECURITY CLASSIFICATION OF REPORT	18. SECURITY CLASSIFICATION OF THIS PAGE	19. SECURITY CLASSIFICATION OF ABSTRACT	20. LIMITATION OF ABSTRACT
Unclassified	Unclassified	Unclassified	